to observe anions with the same metal-carbon composition as for the cation. Based on this fact, as well as the dominant intensity of $Ti_8C_{12}^+$ in Fig. 2 and the nature of the dodecahedral structure, we expect that neutral Ti_8C_{12} would also have a high abundance in the neutral cluster distribution. If our speculation and the proposed model are correct, there are many important implications of the existence of such a stable metallo-carbohedrene. Owing to limitations of our current mass spectrometer, we have not yet been able to mass-analyze ions with masses larger than 1200 amu. However, radio frequency–only operation of our quadrupole mass spectrometer indicates that there are numerous species in the higher mass range.

REFERENCES AND NOTES

1. B. C. Guo, K. P. Kerns, A. W. Castleman, Jr., *J. Phys. Chem.*, in press.
2. H. W. Kroto, J. R. Heath, S. C. O'Brien, R. F. Curl, R. E. Smalley, *Nature* **318**, 162 (1985); R. F. Curl and R. E. Smalley, *Science* **242**, 1017 (1988).
3. W. Weltner, Jr. and R. J. Van Zee, *Chem. Rev.* **89**, 1713 (1989).
4. H. W. Kroto, A. W. Allaf, S. P. Balm, *ibid.* **91**, 1213 (1991).
5. A. F. Hebard *et al.*, *Nature* **350**, 600 (1991).
6. Y. Chai *et al.*, *J. Phys. Chem.* **95**, 7564 (1991).
7. T. Weiske, D. K. Böhme, J. Hrůsák, W. Krätschmer, *Angew. Chem. Int. Ed. Engl.* **30**, 884 (1991); M. M. Ross and J. H. Callahan, *J. Phys. Chem.* **95**, 5720 (1991).
8. T. Guo, C. Jin, R. E. Smalley, *J. Phys. Chem.* **95**, 4948 (1991).
9. B. C. Guo, K. P. Kerns, A. W. Castleman, Jr., in preparation. A standard laser vaporization source, in conjunction with a plasma reactor, was used to produce the cluster, which is analyzed and detected with a quadrupole mass spectrometer. The titration experiments were conducted by mass-selecting the cluster, introducing it into the reaction cell, and detecting the association products with a second quadrupole mass spectrometer.
10. J. P. Collman, L. S. Hegedus, J. R. Norton, R. G. Finke, Eds., *Principles and Applications of Organotransition Metal Chemistry* (University Science Books, Mill Valley, CA, 1987); K. H. Dötz, H. Fischer, P. Hofmann, F. R. Kerissl, U. Schubert, K. Weiss, Eds., *Transition Metal Carbene Complexes* (Verlag Chemie: Deerfield Beach, FL, 1983). T. E. Taylor and M. B. Hall, *J. Am. Chem. Soc.* **106**, 1576 (1984).
11. R. J. Goddard, R. Hoffmann, E. D. Jemmis, *J. Am. Chem. Soc.* **102**, 7667 (1980).
12. F. P. Pruchnik, Ed., *Organometallic Chemistry of the Transition Elements* (Plenum, New York, 1990).
13. L. A. Paquette, R. J. Ternansky, D. W. Balogh, G. Kentgen, *J. Am. Chem. Soc.* **105**, 5441 and 5446 (1983).
14. S. Q. Wei, Z. Shi, A. W. Castleman, Jr., *J. Chem. Phys.* **94**, 3268 (1991); X. Yang and A. W. Castleman, Jr., *J. Phys. Chem.* **94**, 8500 (1990); *ibid.*, p. 8974.
15. H. W. Kroto, *Nature* **329**, 530 (1987).
16. P. Maslak, unpublished work.

17. We thank G. L. Geoffroy, P. Maslak, M. Natan, J. Brauman, and Z. Chen for helpful discussions. Financial support from the U.S. Department of Energy, grant DE-FG02-88-ER60668, is gratefully acknowledged. Initial experiments on the reactions were commenced with support by E. I. du Pont de Nemours through an unrestricted grant to the Department of Chemistry at Pennsylvania State University and the Environmental Protection Agency, grant R-817437-01-0.

12 February 1992; accepted 19 February 1992

Extraction and STM Imaging of Spherical Giant Fullerenes

LOWELL D. LAMB,* DONALD R. HUFFMAN, RICHARD K. WORKMAN, SAM HOWELLS, TING CHEN, DROR SARID, RONALD F. ZIOLO

High-temperature, high-pressure extracts of soot produced by the Krätschmer-Huffman technique (KH carbon) were characterized by mass spectrometry and imaging with scanning tunneling microscopes (STMs). The mass spectra of these samples are similar to those of ambient-pressure, high-boiling-point solvent extractions, supporting the idea that solvent temperature and possibly pressure are key parameters in extraction of the giant fullerenes. The STM images show that the giant fullerenes in these samples are roughly spherical in shape and range in diameter from approximately 1 to 2 nanometers, corresponding to fullerenes containing 60 to 330 atoms. No evidence of bucky tubes was found.

RECENT REPORTS (*1, 2*) OF THE EXtraction from KH-carbon and mass-spectroscopic characterization of the so-called giant fullerenes (C_n, $n \gtrsim 100$) have sparked considerable interest in their properties. These mass spectra, along with some intriguing transmission electron microscopy images published by Wang and Buseck (*3*) and Iijima (*4*), have given rise to speculations that the canonical form of the giant fullerenes is the bucky tube. In the simplest case (*5*), the wall of such a structure is thought to resemble a portion of a single graphitic plane that has been curled until it forms a tube. The tube is capped on each end with a fullerene-like hemisphere, thus leaving no dangling bonds. Before the current work was begun, the sole evidence that seemed to contradict the bucky tube model of the structure of the giant fullerenes was a single STM image published by Wragg *et al.* in a study of solid C_{60}-C_{70} (*6*). This image appeared to show a spherical giant fullerene with a diameter of ~1.5 nm, corresponding to a molecule with 180 to 240 carbon atoms. The authors noted, however, that since this was the only such image to appear in their data set, which contained images of many thousands of smaller fullerenes, identification of this object as a giant fullerene was highly speculative. We report the extraction of giant fullerenes from KH carbon using a low-boiling-point solvent in a high-pressure, high-temperature vessel and STM imaging of these molecules. The images show only spherical giant fullerenes, with no evidence of tubular structures.

In previous work on extraction of the giant fullerenes, high-boiling-point solvents, such as 1,2,3,5-tetramethylbenzene (*1*) or 1,2,4-trichlorobenzene (*2*), were used in standard extraction procedures at ambient pressures. The starting material in these experiments was KH carbon, which previously had been thoroughly washed with low-boiling-point solvents such as toluene (*2*) or benzene followed by pyridine (*1*). The effect of these prior extractions was to remove as much of the readily soluble C_{60} and C_{70} as possible. After the high-temperature extractions, the solvent was removed and mass spectrometry was performed on the residue. Although high-boiling-point solvent, ambient-pressure extractions are quite favorable in terms of solvating the giant fullerenes, these approaches require solvents that are unpleasant to work with and that are hard to remove without heating the sample under vacuum. Also, there is concern that some combination of air, ambient light, and the boiling solution may lead to the formation of unwanted compounds (*2*). These considerations, together with evidence that the key parameter governing extraction of the higher fullerenes under ambient pressure might be the solvent temperature (*2*), and a preliminary report of successful high-pressure, high-temperature xylene extractions of the higher fullerenes (*7*), led us to investigate extractions with toluene at high pressure and temperature.

The starting material was KH carbon (*8*), which had first been solvent-extracted with toluene at ambient pressure to remove as much of the C_{60} and C_{70} as possible. The high-pressure, high-temperature extractions were then carried out in simple pressure bombs built out of 30-cm lengths of 1.2-cm outside-diameter stainless-steel thick-wall tubing, capped on the ends with stainless-steel compression fittings. (Warning: Great care should be used in this procedure, because failure of the vessel may result in an explosion.) Each bomb was loaded with ~5 g of the preextracted KH carbon and ~20 ml of toluene. The bombs were filled to

L. D. Lamb, D. R. Huffman, R. K. Workman, Department of Physics, University of Arizona, Tucson, AZ 85721.
S. Howells, T. Chen, D. Sarid, Optical Sciences Center, University of Arizona, Tucson, AZ 85721.
R. F. Ziolo, Webster Research Center, Xerox Corporation, Webster, NY 14580.

*To whom correspondence should be addressed.

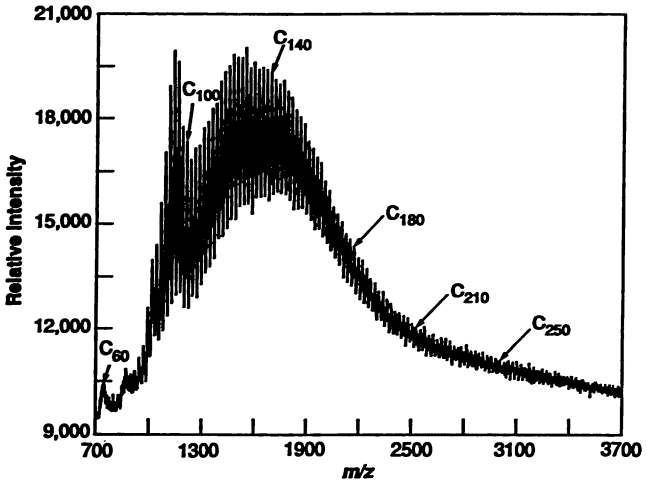

Fig. 1. Time-of-flight mass spectrum of fullerenes prepared by high-pressure bomb extraction of KH carbon with toluene, showing C_{60} and large amounts of higher molecular weight fullerenes up to at least cluster size C_{290}.

capacity, thus excluding as much air as possible. They were then placed in a furnace and heated for 7 hours. After the bombs had cooled, the contents were filtered and washed with ~500 ml of toluene. The resulting dark brown solution was dried on a watch glass, and the residue was scraped up into a powder. This material was washed at least three times in either ethyl ether or hexane to remove any contaminants. Although furnace temperatures from 230° to 350°C were tried, differences in yields and mass spectra were small. At the higher temperatures, however, along with the extraction of fullerenes, there was an unacceptably large production of hexane-soluble hydrocarbons, probably the result of solvent polymerization. Since there appeared to be no production of these unwanted compounds at 230°C, the results presented here are on samples extracted at that temperature. Because of the high ratio of KH carbon to solvent used when loading the bombs, the solution in the bombs became completely saturated in the course of heating and it was not possible to determine what fraction of the starting KH carbon consists of fullerenes soluble by this technique. The yield from a single extraction was consistently 15 to 20 mg, allowing us to roughly estimate the solubility of these higher fullerenes in toluene to be ~1 mg/ml.

The samples were pressed onto indium foil and analyzed by reflecting time-of-flight mass spectrometry with the detector surface biased at 12 keV for high mass detection. Positive direct ions were observed as a result of irradiating the sample with a near-infrared laser pulse at 1.06 μm with a 5-ns pulse width. The power density was varied over different analyses, but generally was kept within a factor of 2 of 1×10^7 W/cm^2, which is below clear plasma threshold. The mass spectrum (direct ions) of the sample extracted at 230°C in the mass spectral region with mass-to-charge ratios (m/z) from 700 to 4000 (inclusive of C_{60} to C_{330}) is shown in Fig. 1. There is a wide distribution of even-numbered carbon cluster molecules differing by 24 atomic mass units (amu), with the C_{2n} cluster pattern clear until ~3500 amu. No evidence was observed for species composed of other than all-carbon molecules. These results are similar to those obtained by other workers (*1, 2*), who used the high-boiling-point solvent, ambient-pressure extraction technique.

For the STM portion of this study, the dry fullerene samples were first redissolved in toluene. The powder redissolved completely, and hence the distributions of fullerenes in the mass-spectral and STM samples were identical. Small drops of this solution were then applied to clean gold foil substrates. After drying, the samples were loaded into air and ultrahigh vacuum (UHV) STMs. Imaging was performed with mechanically cut Pt-Ir tips and a variety of tunneling currents and bias voltages. The optimal tunneling currents and bias voltages for the air and UHV STMs were 0.2 nA and 300 mV and 0.5 nA and 100 mV, respectively. The STM images show a large number of round structures with diameters varying from about 1 to 2 nm, which we interpret as being images of fullerene molecules. For both the air and the UHV studies, the sample density varied from fractional monolayers to several molecular layers. The image quality exhibited a sample thickness dependence; as the sample became thicker, imaging was more difficult. In the course of examining hundreds of fields of view, thousands of these apparently spherical molecules were observed. In control STM studies of UHV-cleaned gold substrates and on bare gold substrates in air, no structures or irregularities were observed. A representative STM image taken in UHV (Fig. 2A) shows fullerene molecules ranging from those approximately the size of C_{60} to giant fullerene molecules such as the one observed at the lower left corner, which measures almost 2 nm in diameter. As discussed elsewhere (*10*), the mechanism by which fullerenes are imaged by STM is not well understood, and sizes of isolated molecules determined by this method must be treated as approximate. For an isolated molecule, the observed diameter depends upon the orientation of the molecule on the surface, upon the interaction between the surface and the molecule, upon tip characteristics, and upon the details of the density of states of the substrate and the orbitals of the molecule.

In fact, accurate size determination requires a periodic arrangement of similar molecules. For example, Fig. 2B displays four larger fullerenes aligned in a row, whereas Fig. 2, C and D, show cross sections parallel and perpendicular to this row, respectively. The four molecules in Fig. 2, B to D, were initially separated from each other and in the course of scanning were pushed together into the arrangement shown. This observation effectively rules out the possibility that this structure is actually a bucky tube, and the image only appears to be made up of four balls because of an STM artifact. The fact that the apparent heights are smaller than the expected molecular diameters is interpreted as arising from the different extent of the wave functions of the molecules and of the substrate. From the cross section shown in Fig. 2C, where the circles denote the large fullerenes, we find that the periodicity gives a diameter of 13.3 (± 0.9) Å.

Since the periodicity of the structure is expected to be uninfluenced by tip-related effects, and because the molecules pack as van der Waals spheres, the nearest-neighbor spacings will be very close to the real size of the molecules. We can estimate the number of carbon atoms, n, in a fullerene molecule by using the simple scaling equation $n \simeq 60\,[(D - 3.4)/7.1]^2$, where D is the measured fullerene size, 7.1 is the cage diameter (*9*), and 3.4 is the difference in size between the van der Waals sphere and the cage diameter, all measured in angstroms. Setting $D = 13.3$ Å for the fullerene molecules shown in Fig. 2C roughly corresponds to C_{120}, whereas a diameter of 20 Å suggests a C_{330} molecule. From Fig. 2D, which is a cross section perpendicular to the row of the four C_{120} molecules, we find a height of only 6 Å, smaller than expected but consistent with previous C_{60} height measurements (*10*). The disparity in height may be due to a difference in the local density of states between the fullerenes and the gold substrate, which could cause the tip to approach the fullerene more closely

than the substrate. All of the observed fullerene molecules were essentially round, and no tube-shaped structures were observed.

The most important result of this work is the absence of any evidence of bucky tubes in our samples. All of the fullerenes examined, which numbered in the thousands, were roughly spherical in shape, regardless of size. Because of the sample size, and because of the considerations discussed above, it is unlikely that this finding is due to an STM artifact or to improper sampling. There are several obvious possible explanations for this finding. One is that tubes simply do not form in the Krätschmer-Huffman technique, and that an approximately spherical shape is preferred. Another explanation for the absence of bucky tubes in our samples is that both tubes and spheres are present in the KH carbon, but that only the spheres are soluble and extracted in the high-pressure, high-temperature extraction technique. If so, this technique offers an extremely selective and efficient method of isolation. It is also possible that bucky tubes are actually produced in the Krätschmer-Huffman process but are reconfigured to spherical molecules during the extraction. In this case as well, such a conversion mechanism would have to be extremely efficient, given the sample size in our study. Another possibility is that bucky tubes are indeed present in our sample, but that they cannot be imaged with STM because they are highly mobile on the substrate and are pushed aside by the tip. This explanation seems highly unlikely, however, since the substrate contact area would be greater for a tube than it would be for an equivalent sphere, and hence one would expect that the tube would adhere to the substrate more strongly than a sphere.

From the analysis that has been done so far on the STM data, it is not possible to tell if the giant fullerenes are hollow; there may be smaller fullerenes or other structures nested inside them. Because of the difficulty in assigning accurate diameters to isolated molecules based on STM images, as discussed above, and because of possible systematic biases in the mass spectra (such as differences in ionization efficiencies of the various fullerenes), it is not possible to confidently correlate the distribution of STM image

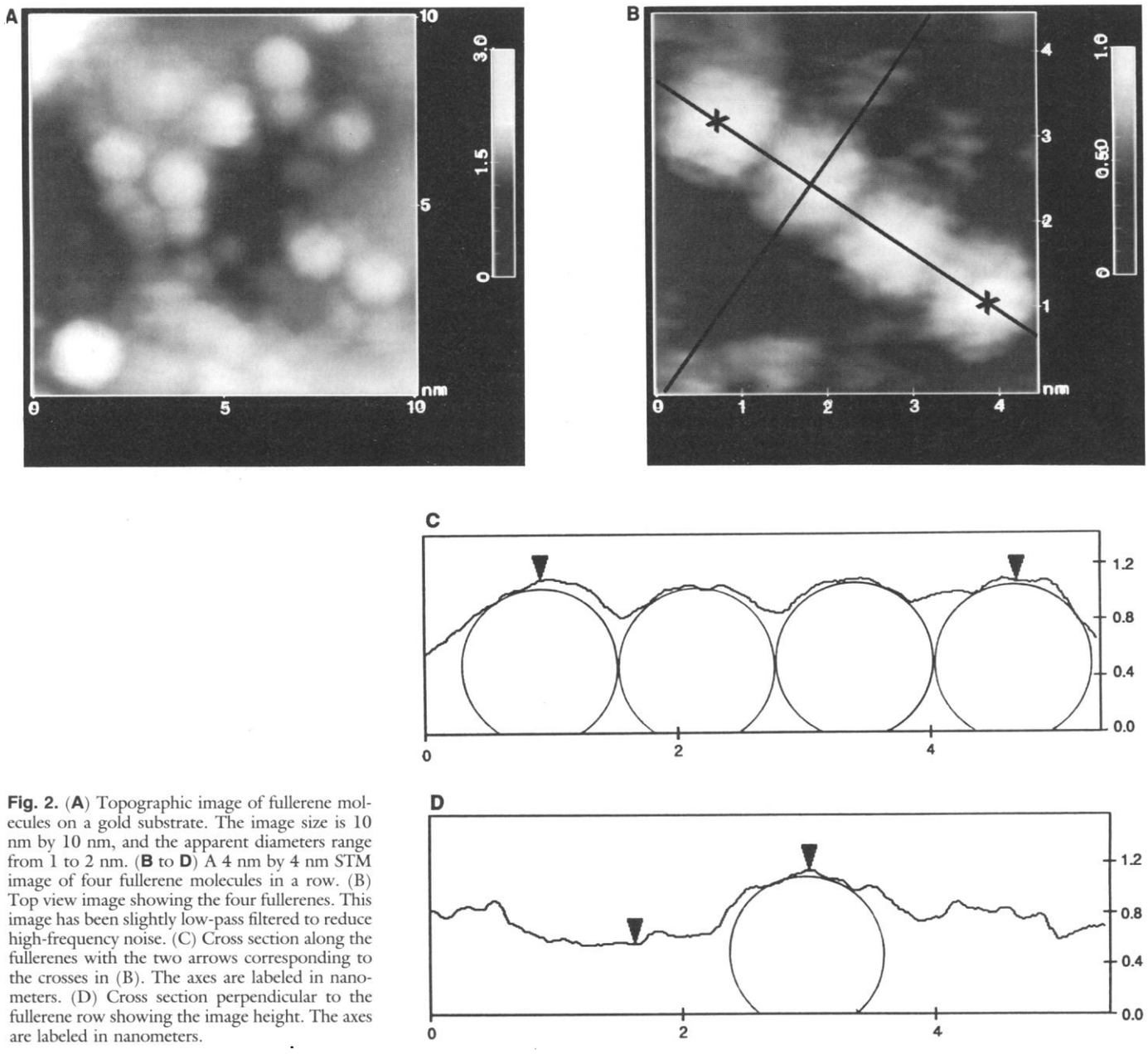

Fig. 2. (**A**) Topographic image of fullerene molecules on a gold substrate. The image size is 10 nm by 10 nm, and the apparent diameters range from 1 to 2 nm. (**B** to **D**) A 4 nm by 4 nm STM image of four fullerene molecules in a row. (B) Top view image showing the four fullerenes. This image has been slightly low-pass filtered to reduce high-frequency noise. (C) Cross section along the fullerenes with the two arrows corresponding to the crosses in (B). The axes are labeled in nanometers. (D) Cross section perpendicular to the fullerene row showing the image height. The axes are labeled in nanometers.

diameters with the mass spectra. Another important question raised by these results is that of the degree of sphericity of the various giant fullerenes, which requires further investigation.

REFERENCES AND NOTES

1. D. H. Parker *et al.*, *J. Am. Chem. Soc.* **113**, 7499 (1991).
2. C. Smart *et al.*, *Chem. Phys. Lett.*, in press.
3. S. Wang and P. R. Buseck, *ibid.* **182**, 1 (1991).
4. S. Iijima, *Nature* **354**, 56 (1991).
5. J. W. Mintmire, B. I. Dunlap, C. T. White, *Phys. Rev. Lett.* **68**, 631 (1991).
6. J. L. Wragg, J. E. Chamberlain, H. W. White, W. Krätschmer, D. R. Huffman, *Nature* **348**, 623 (1990).
7. R. S. Ruoff, T. Randolph, W. R. Creasy, unpublished results.
8. W. Krätschmer, L. D. Lamb, K. Fostiropoulos, D. R. Huffman, *Nature* **347**, 354 (1990).
9. R. Disch and J. M. Schulman, *Chem. Phys. Lett.* **125**, 465 (1986).
10. T. Chen *et al.*, *J. Vac. Sci. Technol. B* **9**, 2461 (1991).

11. We thank R. S. Ruoff for suggesting the use of high-pressure vessels for high-temperature extractions, C. Becker for providing the mass spectral data, and D. Lichtenberger and Q. Fernando for valuable discussions. One of us (D.S.) also thanks the Air Force Office of Scientific Research, the Office of Naval Research, and the Joint Services Optical Program for partial support of this work. The STMs used in these experiments were supplied by Digital Instruments Inc. and McAllister Technical Services.

24 January 1992; accepted 21 February 1992

Surface Charge–Induced Ordering of the Au(111) Surface

JIA WANG, ALISON J. DAVENPORT, HUGH S. ISAACS, B. M. OCKO*

Synchrotron surface x-ray scattering (SXS) studies have been carried out at the Au(111)/electrolyte interface to determine the influence of surface charge on the microscopic arrangement of gold surface atoms. At the electrochemical interface, the surface charge density can be continuously varied by controlling the applied potential. The top layer of gold atoms undergoes a reversible phase transition between the (1 × 1) bulk termination and a (23 × $\sqrt{3}$) reconstructed phase on changing the electrode potential. In order to differentiate the respective roles of surface charge and adsorbates, studies were carried out in 0.1 M NaF, NaCl, and NaBr solutions. The phase transition occurs at an induced surface charge density of 0.07 ± 0.02 electron per atom in all three solutions.

THE UTILIZATION OF SXS, SCANNING tunneling microscopy (STM), and atomic force microscopy techniques during the past decade has greatly enhanced our understanding of surfaces in vacuum. These same techniques are also being used to study electrode surfaces on an atomic scale with an increasing level of sophistication (*1–5*). We report the principal results of a comprehensive SXS study of the Au(111) electrode surface in aqueous electrolytes. In an SXS measurement the diffracted intensity distribution couples directly to the periodicity of the top several layers of metal atoms so that the phase behavior versus the applied potential can be measured directly with a high degree of accuracy. The phase behavior of the Au(111) electrode versus the induced surface charge exhibits universal behavior, independent of the solution species. These findings may have general applicability to vacuum and electrochemical surfaces.

The vacuum atomic arrangement of Au atoms at the Au(111) surface has been obtained from STM measurements (*6, 7*) and from a variety of diffraction techniques including low-energy electron diffraction (LEED) (*8, 9*), transmission electron diffraction (*10*), He scattering (*11*), and SXS (*12, 13*). The observed diffraction peaks have been interpreted as indicating a rectangular (23 × $\sqrt{3}$) unit cell corresponding to a uniaxial compression (4.4%) along the <1,0,0> direction (hexagonal coordinates) (Fig. 1A). Recent SXS (*12*) and STM studies (*6*), in vacuum, have revealed that the direction of the uniaxial compression rotates by ±60° to form a regular array of kink dislocations.

The possibility that Au surfaces might reconstruct under electrochemical conditions was postulated on the basis of the hysteresis in capacity-potential curves (*14, 15*). Ex situ LEED studies have shown that the Au(111) surface, after emersion from an electrochemical cell, forms a (23 × $\sqrt{3}$) phase in the negative potential regime (*16*). Recently, second-harmonic generation (SHG) measurements (*17, 18*) have demonstrated that the phase transition between the (23 × $\sqrt{3}$) phase and the (1 × 1) phase can be monitored in situ by the additional symmetry pattern in the SHG intensity associated with the uniaxial compressed phase. However, it is difficult to extract detailed structural information from ex situ and SHG studies. Concurrent with the present SXS study, in situ STM studies (*19, 20*) in $HClO_4$ solutions have confirmed the existence of the (p × $\sqrt{3}$) reconstruction within the negative potential regime. The precision in this SXS study of the Au(111) electrode is beyond the capabilities of any of the previous probes. The experimental approach is described in (*4, 21, 22*). The applied potential is referenced to an Ag/AgCl(3 M KCl) electrode.

In a surface diffraction measurement, the (p × $\sqrt{3}$) reconstruction gives rise to additional in-plane reflections beyond the underlying (1 × 1) reflections. As demonstrated (*9*), the reconstruction reflections are arranged in a hexagonal pattern surrounding the integer (H, K) positions (Fig. 1B). In Fig. 1C, equal intensity contour lines are shown in the vicinity of the (0,1) reflection for a 0.01 M NaCl solution at −0.3 V. Four reflections surrounding the (0,1) reflection are arranged in a hexagonal pattern, where δ is the length of a hexagonal side (dimensionless units). This pattern is consistent with a (23 × $\sqrt{3}$) unit cell without the additional features expected for a regular array of discommensuration kinks (*12*). At the most positive applied potentials, the reconstruction peaks coalesce at the integer positions.

We investigated the potential dependence of the diffraction pattern by measuring the scattering profile through the (0,1) reflection along the <1,1> direction (Fig. 1C). Along this axis (defined as q_r) the scattering wave vector is given by ($q_r/\sqrt{3}$, 1 + $q_r/\sqrt{3}$). In Fig. 2A, the measured scattering intensity is shown at a series of decreasing potentials between 0.1 and −0.8 V in a 0.01 M NaCl solution. At potentials of 0.10 V and above, the scattering is centered at q_r = 0, which indicates that the surface is not reconstructed. As the potential is reduced below 0.05 V, a second peak emerges, corresponding to the reconstructed phase (see Fig. 1C). Concomitantly, the (0,1) reflection decreases in intensity. The peak position of the reconstruction, ($\delta/\sqrt{3}$, 1 + $\delta/\sqrt{3}$), moves outward (increased compression), and the peak sharpens (increased order) as the potential is decreased.

In order to extract the stripe separation p, the scattering profiles have been described as the sum of two Lorentzians (*21*) (centered at zero and δ). Fits to the Lorentzian form (solid lines in Fig. 2A) describe most of the

J. Wang and B. M. Ocko, Department of Physics, Brookhaven National Laboratory, Upton, NY 11973.
A. J. Davenport and H. S. Isaacs, Department of Applied Science, Brookhaven National Laboratory, Upton, NY 11973.

*To whom correspondence should be addressed.